Excellence of sol-gel engineered Cr₂O₃ and CeO₂-Cr₂O₃ nanocomposite as an efficient electrode for superior capacitive performance

S. R. Shafqat ^a, A. Arshad ^a, S. Bano ^a, I. Arif ^a, S. Mazher ^a, Z. A. Sandhu ^b, M. Danish ^a, M. S. Youssef ^c, H. T. Ali ^c, M. A. Raza ^{b, *}

A major concern of current world is deficit in energy sector and renewable energy sources. Researchers are investigating serval materials to fulfil the energy demands with efficient manners. In this regard, TMOs based composites are under consideration for the effective energy storage system. In this study, Pure Cr₂O₃ and CeO₂-Cr₂O₃ was prepared via modified sol-gel methodology. The prepared nanocomposites were investigated for superior capacitive performance. The structural and X-ray analysis of prepared composite materials was performed via scanning electron microscope (SEM) and X-ray diffraction spectroscopy (XRD), respectively. The SEM analysis of CeO₂-Cr₂O₃ revealed interconnected uniform distribution of CeO2 into Cr2O3 matrix ensures higher surface area and active site accessibility. Similarly, XRD analysis confirm the successful formation of orthorhombic nanocrystal structure. The prepared nanocomposites were investigated for Supercapacitor application. The cyclic voltammetry (CV) demonstrated excellent specific capacitance and energy density value of 1063 F/g and 36.92 Wh/kg, respectively. The superior CeO₂-Cr₂O₃ electrode material was also investigated for cycling performance. The nanocomposite showed excellent retention of 92.43% at 100th cycles. The cycling performance and capacitive efficiency recommends this material for energy storage system.

(Received June 25, 2025; Accepted October 1, 2025)

Keywords: Nanomaterials, Sol-gel, Energy crises, Binary composites, Super capacitor

1. Introduction

One of the most topical problems of the modern world is future global energy crisis [1]. The population growth rate and high level of energy demand, coupled with negative environmental effects have enforced researchers to reconsider valuable energy sources and sustainable alternative solutions [2]. One of the most promising ones is the development of renewable sources of energy coupled with effective energy storage systems [3]. The energy storage devices like capacitors and batteries have been important in this quest of energy storage [4]. However, batteries have high energy density and are commonly used while capacitors have high power density. Meanwhile, both are limited by low energy density of capacitors and low power density of batteries, as well as by restricted life cycle and safety [5]. Supercapacitor have been emerged as the next-door technology in energy storage to solve energy problems. It exhibited distinctive features such as rapid charging/discharging, higher power density, long cycle life, and stability [6]. Supercapacitor are divided into electrochemical charge-storing type (electrochemical double-layer capacitors or EDLCs) and pseudocapacitors depending on the charge-storage mechanism [7]. EDLCs are based on separation of charge physically at the interface of electrode-electrolyte whereas pseudocapacitors use faradaic redox procedures using metal oxides (MOs) leading to increased energy storage [8].

^a Department of Chemistry, Faculty of Science, University of Sialkot, Sialkot, 51310, Pakistan

^b Department of Chemistry, Faculty of Science, University of Gujrat, Hafiz Hayat Campus, Gujrat, 50700, Pakistan

^c Department of Mechanical Engineering, College of Engineering, Taif University, Kingdom of Saudi Arabia

^{*} Corresponding authors: asamgcu@yahoo.com https://doi.org/10.15251/DJNB.2025.204.1167

Transition metal oxides have been attracted due to demonstration of numerous redox states, therefore, promoting accelerated redox reactions, and representing lower to higher capacitance [9]. Hybrid electrode materials design is often based on the constituent materials like MnO₂, RuO₂, and transition metal hydroxides like the Ni, Co, and Cu-based compounds are usually employed to increase energy storage [10]. Such hybrids sustain high energy density and quick charge transfer which is perfect in high performance Supercapacitor.

The TMOs can be prepared with a range of techniques such as hydrothermal [11], sol-gel [12], co-precipitation [13], chemical vapour deposition [14], and electrospinning [14], etc. The solgel method is unique among them and is preferred because it is simple, uses a low processing temperature, affordable, can achieve control over material composition and morphology on a molecular scale [15]. Chromium oxide, one of the most popular and renowned transition metal oxides, due to its number of valence states and electrochemical stability. It has good redox properties, high conductivity and chemical stability so that it has potential to be used as capacitor electrode material [16]. Another rare-earth oxide promising to use is cerium oxide (CeO₂), which has variable oxidations (Ce⁴⁺/Ce³⁺) and has high oxygen storage capacity [17]. Nonetheless, its average capacitance resists its alone utilization in Supercapacitor. CeO₂, together with chromium, develops a composite that addresses such shortcomings. The addition of chromium raises oxygen vacancies, raises lattice oxygen mobility and raises Ce⁴⁺/Ce³⁺ redox activity [18].

There is also the advantage of two redox mechanisms (Ce⁴⁺/Ce³⁺ & Cr³⁺/Cr⁶⁺) that provide larger number of active sites of the charge transfer. Furthermore, structural integrity provided by Cr enhances the sustainability especially in long electrochemical cycle thereby providing reliable long term performance [19]. Cr-doped ceria has been investigated as an electrode material for Supercapacitor by Ghosh et.al. which demonstrated Cr-doped CeO₂ based materials had an aerial capacitance of 4.46 mF/cm² at current density of 0.8 mA/cm². The good stability of the device was demonstrated with a capacitance loss of only 20 percent after 10,000 charge discharge cycle [20].

The present work aim to prepare and examine the electrochemical performance of sol-gel engineered Cr₂O₃ and CeO₂-Cr₂O₃ nanomaterials as a Supercapacitor electrode material. This study showed that these composites CeO₂-Cr₂O₃ have been rarely documented with superior capacitive performance. The synthesis of these nanocomposites for energy storage system will really a valuable step towards sustainable energy goals.

2. Experimental work

2.1. Material used

The preparation of pure CeO_2 and CeO_2 - Cr_2O_3 nanocomposites were prepared via employing various reagents and precursor salts. The cerium sulphate tetra hydrated $(Ce(SO_4)_2 \cdot 4H_2O)$, and chromium nitrate hexahydrated $(Cr(NO_3)_3 \cdot 6H_2O)$ was utilized as precursor salts with 99 % purity. The salts used were purchased from sigma Aldrich with high purity. The sodium dodecyl sulfate $(NaC_{12}H_{25}SO_4)$ used as surfactant that may facilitated in gel formation. Additionally, the ethanol (C_2H_5OH) was used in nickel foam as working electrode preparation. All the salts were used as purchased from the aforementioned company without and further purification or alterations.

2.2. Synthesis of pure CeO₂ nanomaterial

A modified or optimized sol-gel methodology was employed for the synthesis of pure cerium oxide (CeO₂) nanomaterial [21]. A 0.863 g of 0.6 M chromium nitrate hexahydrated (Cr(NO₃)₃.6H₂O) was weighed and added into distilled water. The chromium salt with water placed on heating plate with stirring of 600-650 rpm at 35°C for 15-20 min. After continuous stirring, the complete salt solubilized in the distilled water and a clear solution was appeared. Followed by homogenization, a specific amount of sodium dodecyl sulfate that act as a surfactant was added in the above solution till the formation of gel. The prepared gel later dried in the oven at 300 °C for 20 min. The dried gel then crushed into fine powder and calcination of material was performed as a final step for the preparation of nanomaterials. The fine powder again placed in the oven for

calcination at 500 °C for 5 h. Finally, the calcined material crushed and convert into fine powder. The prepared material then used for characterizations owing to confirm its structural morphology.

2.3. Synthesis of CeO₂-Cr₂O₃ nanocomposites

The CeO₂-Cr₂O₃ nanocomposite was prepared using same procedure with varying amount of precursor salts. For the preparation of cerium-chromium composite, 0.731 g of cerium sulphate tetra hydrated (Ce(SO₄)₂·4H₂O), and 0.798 g of chromium nitrate hexahydrated (Cr(NO₃)₃.6H₂O) was added into distilled water. The salts of both metals homogenized in the distilled water with consistent stirring. The above procedure was repeated for the preparation of nanocomposite material.

3. Results and discussion

3.1. Characterization

The X-ray diffraction patterns of Cr_2O_3 and CeO_2 - Cr_2O_3 are shown in figure 1. The CeO_2 - Cr_2O_3 XRD graph confirmed the successful formation of orthorhombic nanocrystal structure. This is quite evident that CeO_2 - Cr_2O_3 material exhibited formation of a composite phase by interaction between cerium oxide, (CeO_2) and chromium oxide, (Cr_2O_3) . The diffraction patterns identified in the XRD corresponding to JCPDS cards 00-34-0394 and 00-038-1479. The typical reflections corresponding to JCPDS # 00-34-0394, i.e., $2\theta = 30^{\circ}$ (111), 31 (200), 49° (220), 56.3° (311), 59° (222), 75° (331) and 78° (420) are readily visible and matched quite well with standard pattern for cerium oxide clearly [22-25].

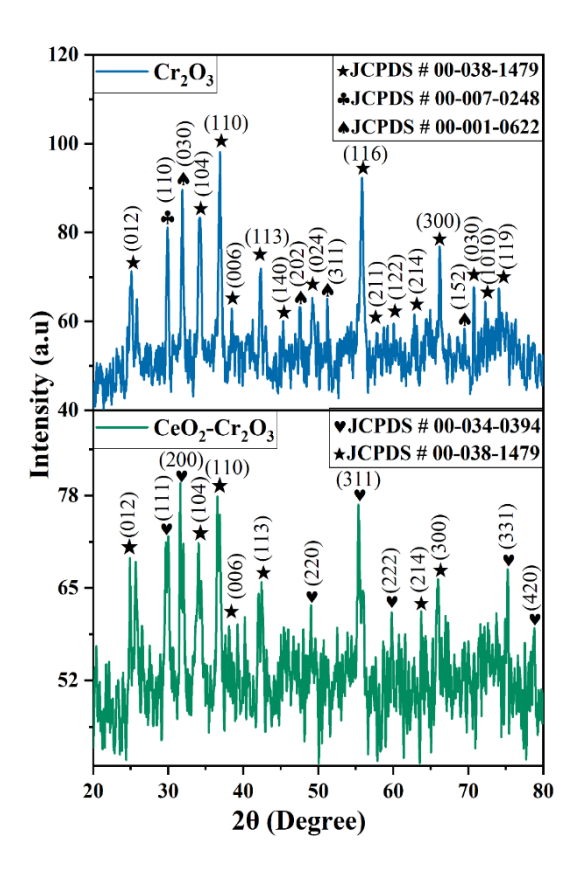


Fig. 1. XRD Spectra of prepared Cr_2O_3 and CeO_2 - Cr_2O_3 nanocomposites.

Similarly, reflection peaks of chromium oxide corresponding to JCPDS # 00-038-1479, such as planes at $2\theta = 24.9^{\circ}$ (012), 34.6° (104), 36° (110), 38° (006), 42° (113), 63° (214) and 65.90° (300) ensure the synthesis of chromium oxide [26, 27]. The co-existence of these different

diffraction peaks indicating both phases of CeO_2 and Cr_2O_3 , confirms the formation of a newly mixed oxide, indicating a successful structural integration at crystalline level. Conversely, the XRD spectrum of pure Cr_2O_3 nanomaterial showed a multiphase crystalline structure as evidenced with the help of three distinct JCPDS profile cards # 00-038-1479,00-007-0248, 00-001-0622. The major phase was defined as rhombohedral α - Cr_2O_3 corresponding to JCPDS # 00-038-1479, which was proved by sharp peaks of (012), (104), (110), (006), (113), (140), (024), (116), (211), (122) (214), (300), (030), (1010) and (119) planes [28-30]. These peaks denote a well crystallized high-purity phase. Further assumption of JCPDS # 00-007-0248 [31], (110), indicate the existence of a secondary Cr_2O_3 phase, with minor structural irregularities caused by a possibility of nanoscale grain borders or other orientations. In addition, there are small peaks agreeing with JCPDS # 00-001-0622; mainly (030), (202), (311), and (152) which signifies that there is a tertiary phase, probably a small amount of intermediate chromium oxides or some structural variation produced due to synthesis conditions [32, 33].

The Fourier transform infrared spectroscopy was employed for the determination of functional group identification in prepared nanomaterials. The CeO₂-Cr₂O₃ binary nanocomposite shows the presence of many characteristic vibrations bands participating in the formation of the successful nanocomposite and strong interaction of the metal oxides. The broad absorption peak in the region 3492 cm⁻¹ was assigned to the O-H stretching vibration, owing to water molecules. The 1620 cm⁻¹ band was the bending vibration of the H-O-H compound, which again ensures the absorbent water (figure 2). A peak in the range of 1164-997 cm⁻¹ my attributed to C-O stretching vibration within residual [34, 35]. A notable absorption band was observed at 536 cm⁻¹ could be corresponding to the cerium oxide [34, 36]. Moreover, a higher absorption band of 1630 cm⁻¹ is attributed to adsorbed water molecules in Cr₂O₃ spectrum [37]. The other strong peak at 616 cm⁻¹ is related to Cr-O stretching vibrations and it confirms the existence of chromium oxide [38]. The other peaks in the range of 1164 -997 cm⁻¹ are typical of Cr oxide especially when Cr-O bonds occur in tetrahedral units or when chromate species happen to be surface bound [39, 40]. This band is common in both spectra indicates the presence of Cr-O vibrations in binary phase of nanocomposites as well.

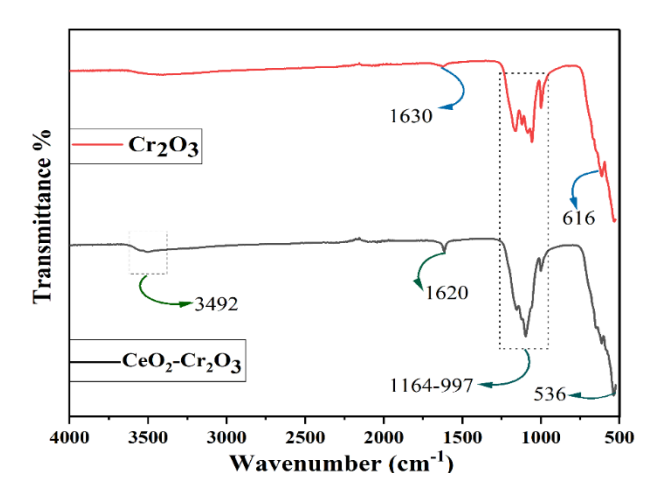


Fig. 2. FTIR Spectrum of prepared pure Cr_2O_3 and CeO_2 - Cr_2O_3 nanocomposites.

The scanning electron microscopy analysis depicted crucial insight about morphological and structural distinctions between pure Cr₂O₃ as shown in figure 3 (a, b) and the CeO₂-Cr₂O₃ nanocomposite figure 3 (c, d). The pure Cr₂O₃ demonstrated irregular sharp-edged nanoparticles with a scattered porous structures and flaky structural morphology, suggesting reduced interconnectivity of particle and restricted surface area. Conversely, the CeO₂-Cr₂O₃ nanocomposite depicts a considerably modified structural morphology in which particles of CeO₂ seem uniformly distributed over the matric of Cr₂O₃. This structural morphology preparing a more cohesive and

denser structure with an evident enhance in pore density and surface roughness. The preparation of interconnected and porous network improves transportation of ions and penetration of electrolyte. These structural improvements are directly corresponding to superior electrochemical excellence of the CeO₂-Cr₂O₃ nanocomposite in Supercapacitor applications.

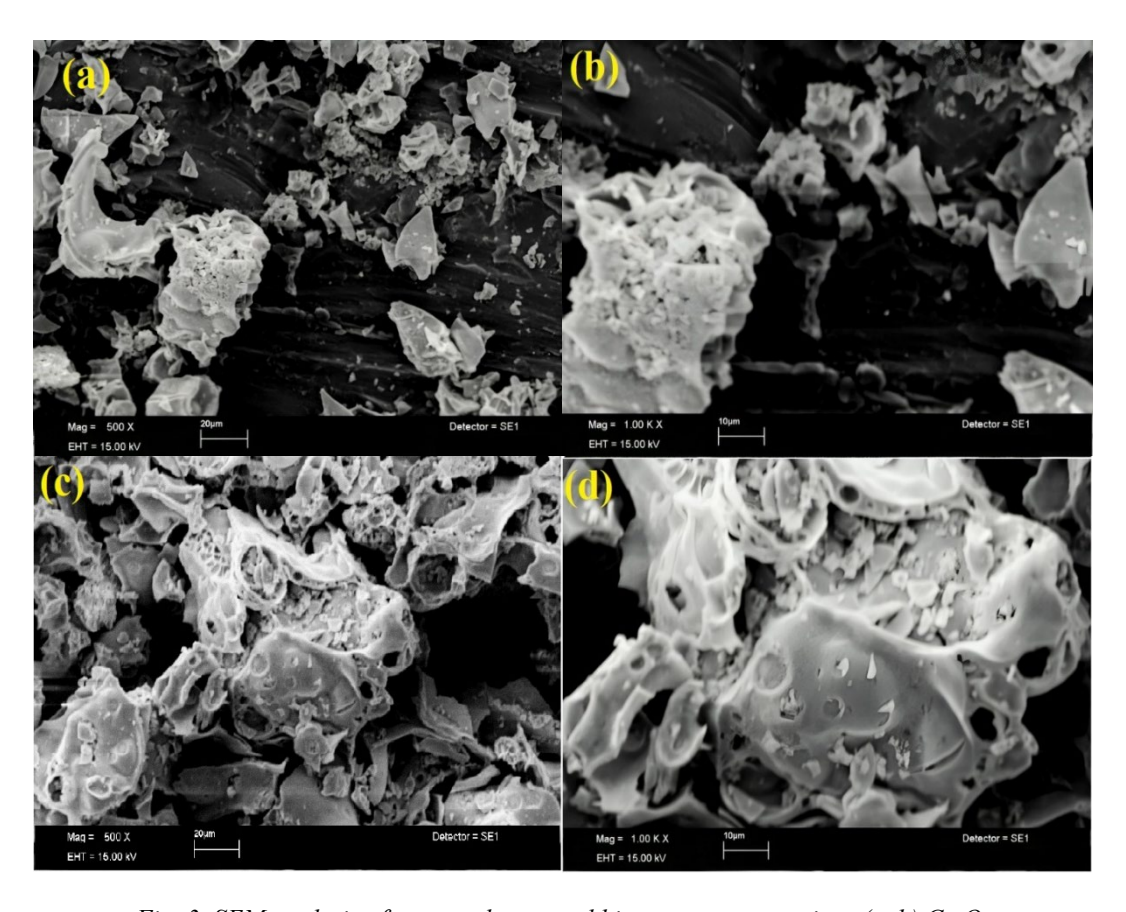


Fig. 3. SEM analysis of prepared pure and binary nanocomposites, (a, b) Cr_2O_3 and (c, d) CeO_2 - Cr_2O_3 nanocomposites.

3.2. Electrochemical performance of pure CeO₂ and CeO₂-Cr₂O₃ nanocomposites

The electrochemical performance of prepared pure CeO₂ and CeO₂-Cr₂O₃ nanocomposites was performed by preparing working electrode on nickel foam. The CV curves were taken at distinct scan rates of 10-200 mV/s in 2M KOH as an electrolytic solution as shown in figure 4. The potential window of CV curves was set at 0.3-0.8 V. The redox reaction in the electrolyte was facilitated by the presence of OH⁻ ions. The symmetrical shapes of CV curves may have attributed to improved conductivity that directly involved in the efficient electron kinetic mechanism. The electrolyte employed in cyclic voltammetry performance was 2M KOH, whose pH was high that stabilize the electrode and take part in the change in redox potential, which ensures the superior capacitive performance of synthesized nanocomposites [41]. The presence of various redox peaks confirmed the electrochemical reactions occur on the surface of electrode [42, 43].

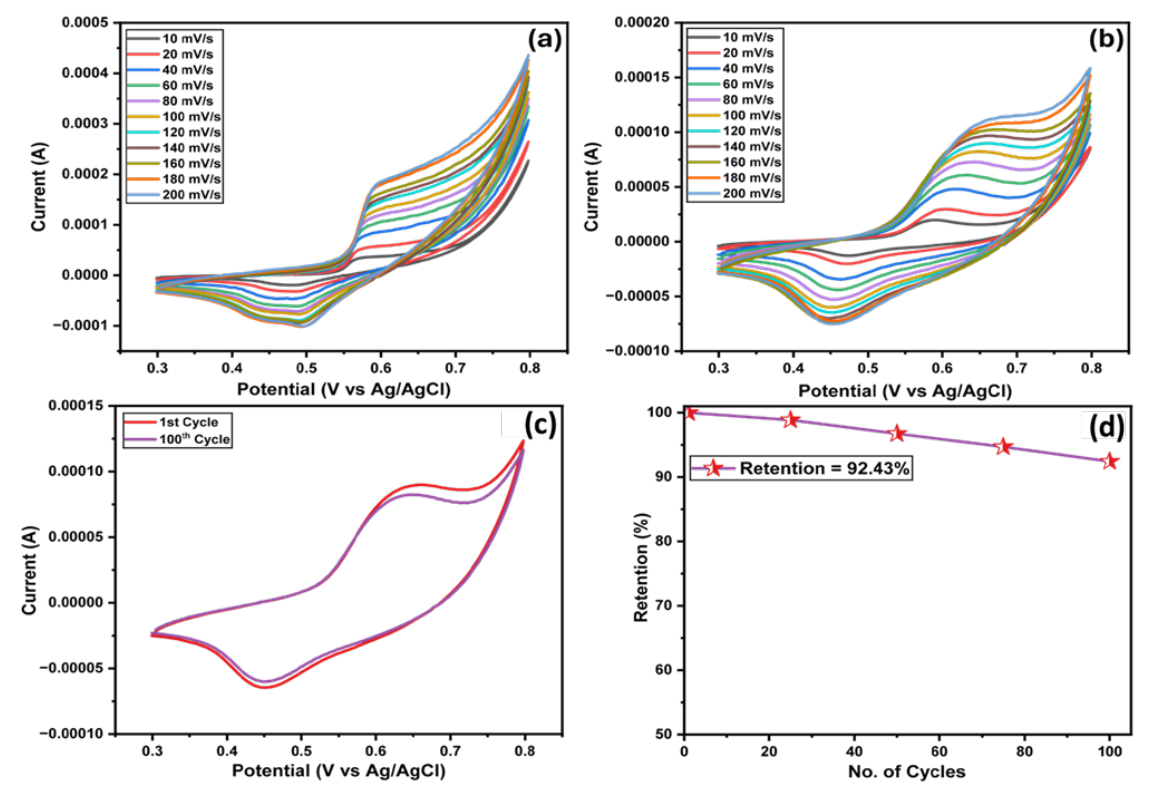


Fig. 4. Cyclic voltammetry performance of prepared pure and binary nanocomposites, (a) CV curves of Cr_2O_3 (b) CV curves of CeO_2 - Cr_2O_3 nanocomposites, (c) cyclic stability of CeO_2 - Cr_2O_3 at 100^{th} cycles and, (d) retention of CeO_2 - Cr_2O_3 nanocomposites.

The CeO₂-Cr₂O₃ nanocomposites illustrated better redox reaction response than pure CeO₂, which ensures its excellent capacitive and energy density performance. The improvement in specific capacitance comprises increase in surface rea and active sites that lower or decline defects in prepared nanocomposite. The specific capacitance from CV can be calculated from given equation 1 [44].

$$C_{sp} = \frac{\int_{V_a}^{V_C} I(V)dV}{mv(V_c - V_a)} \tag{1}$$

where m illustrates electrode active mass, v represents the scan rate and V_c - V_a presented to potential window during CV performance.

Similarly, the energy density of nanocomposite materials were calculated using reported equation 2 [45].

$$E.D = \frac{c_{sp} \times \Delta V^2 \times 1000}{2 \times 60 \times 60}$$
 (2)

The change in CV shape showed with the variation in scan rate. The higher scan rate like 200 mV/s demonstrated transferring of oxidation peaks at higher potential and reduction peaks towards lower potential. The main difference between oxidation and reduction peaks potential showed redox reaction irreversibility. The decrease in specific capacitance at higher scan rates, confirm the uncertainty of internal active sites. At higher scan rate, the electrode surface showed substantial role in charge-discharge process at the time of redox reaction [46].

Moreover, the cycling performance of the best suitable working electrode material CeO₂-Cr₂O₃ was assessed at 100 cycles of CV. The symmetrical shape of redox peaks at 100th cycle ensures the excellent cyclic stability and exceptional retention of material about 92.45%. The composite of Ce in the chromium matrix may increase the porosity and homogeneity of electrode, which relates

to superior electrochemical performance. Moreover, the specific capacitance and energy density of prepared materials were calculated. The pure CeO₂ and CeO₂-Cr₂O₃ nanocomposites showed specific capacitance value of 817 and 1063 F/g, respectively. The CeO₂-Cr₂O₃ electrode material presented excellent capacitance than pure one, owing to synergistic effect of cerium and chromium in composite material as depicted in figure 5. Moreover, the energy density was also calculated about 28.71 and 36.92 Wh/kg for pure CeO₂ and CeO₂-Cr₂O₃ nanocomposites, respectively.

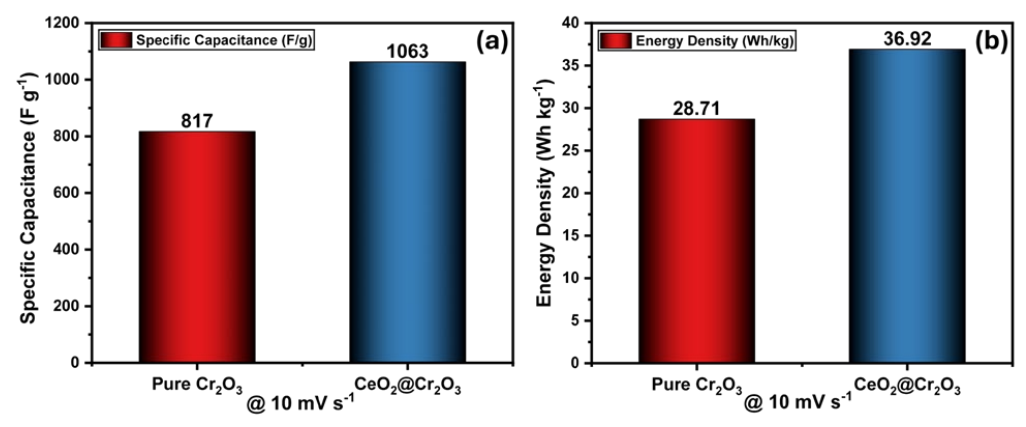


Fig. 5. Specific capacitance and energy density comparison of pure and binary nanocomposites, (a) C_{sp} and E.D of Cr_2O_3 (b) C_{sp} and E.D of CeO_2 - Cr_2O_3 nanocomposites.

The electrochemical impedance spectroscopy was also used for the further validation and electrochemical kinetic mechanism determination of prepared pure CeO₂ and CeO₂-Cr₂O₃ nanocomposites as shown in figure 6. It is a more viable technique excessively used in electrochemical kinetics mechanism [47]. However, the composite material showed remarkable electronic excellence reliability. The EIS analysis particularly Nyquist plot consists of two regions, a semicircle and a straight line. The CeO₂-Cr₂O₃ electrode material presented lower semicircle that probably ensures very limited resistance as compared to the pure CeO₂, suggesting the remarkable transportation of charges at the interface of the electrode/electrolyte.

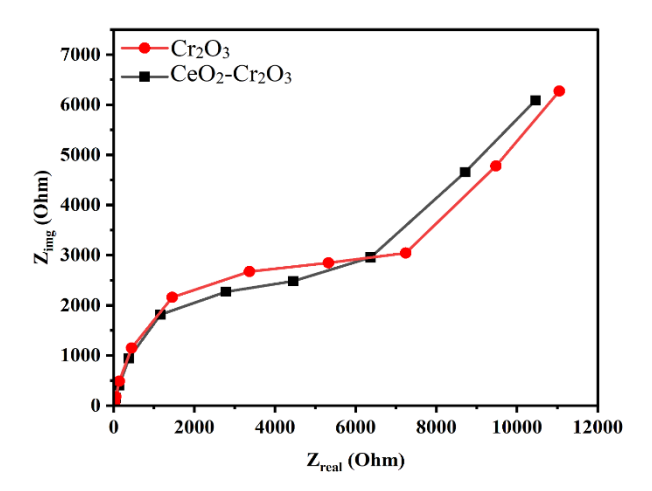


Fig. 6. Electrochemical impedance spectroscopy of pure and binary nanocomposites.

It illustrated that the charge transfers occur at the interface between electrode and electrolyte. The mechanism of charge transfer kinetics improves the surface area and conductivity of CeO₂-Cr₂O₃. The enhance in vertical line segments of composite material showed excellent diffusion of ions in electrolyte. The adsorption process at the surface of electrode confirmed the improved surface area and actives sites that may directly improve electrochemical excellence.

4. Conclusion

A modified sol gel approach was employed for the successful synthesis of pure Cr₂O₃ and CeO₂-Cr₂O₃ nanocomposites. The sodium dodecyl sulphate used as a surfactant in the sol-gel methodology. The prepared materials were investigated with SEM, XRD and FTIR analysis for the confirmation of phase structure, structural morphology and vibrational bands in the prepared nanocomposites, respectively. The prepared nanocomposites were investigated for superior capacitive performance. The SEM analysis of CeO₂-Cr₂O₃ composite material depicted successful formation of material with enhance porosity and interconnected structures. The prepared pure and nanocomposites were investigated for capacitive performance. The cyclic voltammetry demonstrated efficient redox reaction on the surface of electrode material, while electrochemical impedance spectroscopy ensured better ion diffusion kinetic mechanism in nanocomposite material. The pure Cr₂O₃ and CeO₂-Cr₂O₃ electrode materials showed excellent specific capacitance values of 817 F/g and 1063 F/g, respectively. The energy density of both materials was investigated 36.92 and 28.71 Wh/kg, respectively. The CeO₂-Cr₂O₃ nanocomposite demonstrated excellent retention even after consistent cyclic performance.

Data Availability Statement

No additional new data were created.

Conflicts of Interest

The authors declare that they have no known competing financial interests or personal relationships that could have appeared to influence the work reported in this paper.

Acknowledgements

The authors would like to acknowledge Deanship of Graduate Studies and Scientific Research, Taif University for funding this work.

References

- [1] Z.A. Sandhu, Asifa, S.R. Shafqat, M. Danish, K.M. Batoo, M.F. Ijaz, M.A. Raza, S. Ashraf, S. Ghaffar, Ionics (2025) 1-16; https://doi.org/10.1007/s11581-025-06267-4
- [2] I.D. Yadav, A. Ansari, D. Yadav, S.S. Garje, Bulletin of Materials Science 46(2) (2023) 86; https://doi.org/10.1007/s12034-023-02921-7
- [3] H.T. Das, S. Dutta, N. Das, P. Das, A. Mondal, M. Imran, Journal of Energy Storage 50 (2022) 104643; https://doi.org/10.1016/j.est.2022.104643
- [4] Y. Gogotsi, R.M. Penner, ACS Publications, 2018, pp. 2081-2083; https://doi.org/10.1021/acsnano.8b01914
- [5] N. Bibi, Y. Xia, S. Ahmed, Y. Zhu, S. Zhang, A. Iqbal, Ceramics International 44(18) (2018) 22262-22270; https://doi.org/10.1016/j.ceramint.2018.08.348
- [6] Z.A. Sandhu, M. Danish, U. Farwa, M.A. Raza, A.H. Bhalli, A. Sultan, N. Alwadai, W. Mnif, Journal of Inorganic and Organometallic Polymers and Materials (2025) 1-14; https://doi.org/10.1007/s10904-025-03650-6
- [7] N. Maheswari, G. Muralidharan, Energy & Fuels 29(12) (2015) 8246-8253; https://doi.org/10.1021/acs.energyfuels.5b02144
- [8] M. Khot, A. Kiani, International Journal of Energy Research 46(15) (2022) 21757-21796; https://doi.org/10.1002/er.8763

- [9] R. Liu, A. Zhou, X. Zhang, J. Mu, H. Che, Y. Wang, T.-T. Wang, Z. Zhang, Z. Kou, Chemical Engineering Journal 412 (2021) 128611; https://doi.org/10.1016/j.cej.2021.128611
- [10] R. Singhal, M. Chaudhary, S. Tyagi, D. Tyagi, V. Bhardwaj, B.P. Singh, Journal of Materials Research 37(13) (2022) 2124-2149; https://doi.org/10.1557/s43578-022-00598-y
- [11] Z. Wang, Y. Long, D. Cao, D. Han, F. Gu, Electrochimica Acta 307 (2019) 341-350; https://doi.org/10.1016/j.electacta.2019.03.230
- [12] D. Bokov, A. Turki Jalil, S. Chupradit, W. Suksatan, M. Javed Ansari, I.H. Shewael, G.H. Valiev, E. Kianfar, Advances in Materials Science and Engineering 2021(1) (2021) 5102014; https://doi.org/10.1155/2021/5102014
- [13] M. Chaudhary, M. Singh, A. Kumar, Y.K. Gautam, A.K. Malik, Y. Kumar, B.P. Singh, Ceramics International 47(2) (2021) 2094-2106; https://doi.org/10.1016/j.ceramint.2020.09.042
- [14] D. Barreca, E. Fois, A. Gasparotto, C. Maccato, M. Oriani, G. Tabacchi, Molecules 26(7) (2021) 1988; https://doi.org/10.3390/molecules26071988
- [15] M. Parashar, V.K. Shukla, R. Singh, Journal of Materials Science: Materials in Electronics 31(5) (2020) 3729-3749; https://doi.org/10.1007/s10854-020-02994-8
- [16] S. Ghosh, K. Anbalagan, U.N. Kumar, T. Thomas, G.R. Rao, Applied Materials Today 21 (2020) 100872; https://doi.org/10.1016/j.apmt.2020.100872
- [17] R. Kumar, A. Agrawal, R.K. Nagarale, A. Sharma, The Journal of Physical Chemistry C 120(6) (2016) 3107-3116; https://doi.org/10.1021/acs.jpcc.5b09062
- [18] Z. Xue, L. Lv, Y. Tian, S. Tan, Q. Ma, K. Tao, L. Han, ACS Applied Nano Materials 4(3) (2021) 3033-3043; https://doi.org/10.1021/acsanm.1c00161
- [19] V.J. Angadi, K. Abdulvakhidov, N. Lyanguzov, A. Kumar, H. Payal, C. Prakash, B. Pandit, M. Ubaidullah, Journal of Materials Science: Materials in Electronics 35(6) (2024) 420; https://doi.org/10.1007/s10854-024-12107-4
- [20] S. Ghosh, B. Rani, Ionics (2025) 1-8; https://doi.org/10.1007/s11581-025-06199-z
- [21] Z.A. Sandhu, M. Danish, A. Shoaib, S. Ashraf, M. Zain, M. Aslam, K.M. Batoo, M.F. Ijaz, Journal of Inorganic and Organometallic Polymers and Materials (2025) 1-19; https://doi.org/10.1007/s10904-024-03523-4
- [22] P. Shanmugam, G.P. Kuppuswamy, K. Pushparaj, B. Arumugam, A. Sundaramurthy, Y. Sivalingam, Journal of Materials Science: Materials in Electronics 33(12) (2022) 9483-9489; https://doi.org/10.1007/s10854-021-07441-w
- [23] T. Kaur, K. Singh, J. Kolte, Materials Today: Proceedings 80 (2023) 937-941; https://doi.org/10.1016/j.matpr.2022.11.331
- [24] L. Zhang, Y. Shen, ChemElectroChem 2(6) (2015) 887-895; https://doi.org/10.1002/celc.201402432
- [25] S.A. Ar Sayyed, N.I. Beedri, V.S. Kadam, H.M. Pathan, Bulletin of Materials Science 39 (2016) 1381-1387; https://doi.org/10.1007/s12034-016-1279-7
- [26] M. Ishtiaq, D. Ali, R. Ahmad, I. Muneer, F. Bashir, M. Hanif, T.M. Khan, S.A. Abbasi, Surfaces and Interfaces 37 (2023) 102741; https://doi.org/10.1016/j.surfin.2023.102741
- [27] D. Ali, M. Ishtiaq, R. Ahmad, I. Muneer, F. Bashir, M. Hanif, T.M. Khan, S.A. Abbasi, A Comparison of Antibacterial Activity in Dark-Uv Light in Perspective of Surface and Structural Properties of Spray Pyrolysis Grown Cu Doped Cr2o3 Thin Films, Available at SSRN 4259302 [28] M. Kerbstadt, E.M.H. White, M.C. Galetz, Materials 16(23) (2023) 7480;
- https://doi.org/10.3390/ma16237480
- [29] P. Ivanov, S. Watts, D. Lind, Journal of Applied Physics 89(2) (2001) 1035-1040; https://doi.org/10.1063/1.1331343
- [30] D. Domyati, Optical Materials 152 (2024) 115479; https://doi.org/10.1016/j.optmat.2024.115479
- [31] Q. Yao, C. Guo, X. Li, X. Jin, G. Lu, X. Yi, W. Huang, Z. Dang, Geochimica et Cosmochimica Acta 329 (2022) 70-86; https://doi.org/10.1016/j.gca.2022.05.018

- [32] Z. Alexzman, N. Salamun, M. Ibrahim, S. Sidi, N. Annuar, Journal of Environmental Chemical Engineering 12(3) (2024) 112531;
- https://doi.org/10.1016/j.jece.2024.112531
- [33] N.H. Rozali Annuar, Z.A. Alexzman, N. Salamun, M.L. Ibrahim, Catalytic Hydrogenolysis of Sorbitol to Glycols Over Chromium Oxide Silica, Available at SSRN 4611813 (2023); https://doi.org/10.2139/ssrn.4611813
- [34] B. Jain, A.K. Singh, A. Hashmi, M.A.B.H. Susan, J.-P. LelloucheAdvanced Composites and Hybrid Materials 3 (2020) 430-441;
- https://doi.org/10.1007/s42114-020-00159-z
- [35] A.L. Khan, Dhanjai, R. Jain, Journal of Applied Electrochemistry 50(6) (2020) 655-672; https://doi.org/10.1007/s10800-020-01418-z
- [36] K.S. Agrawal, V.S. Patil, A.G. Khairnar, A.M. Mahajan, Journal of Materials Science: Materials in Electronics 28 (2017) 12503-12508; https://doi.org/10.1007/s10854-017-7072-6
- [37] D. Scarano, A. Zecchina, S. Bordiga, G. Ricchiardi, G. Spoto, Chemical Physics 177(2) (1993) 547-560; https://doi.org/10.1016/0301-0104(93)80032-5
- [38] B. Sone, E. Manikandan, A. Gurib-Fakim, M. Maaza, Green Chemistry Letters and Reviews 9(2) (2016) 85-90; https://doi.org/10.1080/17518253.2016.1151083
- [39] B.B. Kamble, M. Naikwade, K. Garadkar, R.B. Mane, K.K.K. Sharma, B.D. Ajalkar, S.N. Tayade, Journal of Materials Science: Materials in Electronics 30 (2019) 13984-13993; https://doi.org/10.1007/s10854-019-01748-5
- [40] M. Tsegay, H. Gebretinsae, Z. Nuru, Materials Today: Proceedings 36 (2021) 587-590; https://doi.org/10.1016/j.matpr.2020.05.503
- [41] M. Danish, Z.A. Sandhu, S. Sharif, M.A. Raza, M. Elahi, M. Aslam, M. Zain, K.M. Batoo, M.F. Ijaz, Journal of Inorganic and Organometallic Polymers and Materials (2024) 1-21; https://doi.org/10.1007/s10904-024-03455-z
- [42] R. Ahmed, G. Nabi, F. Ali, F. Naseem, M.I. Khan, T. Iqbal, M. Tanveer, W. Ali, N.S. Arshad, A. Naseem, Materials Science and Engineering: B 284 (2022) 115881; https://doi.org/10.1016/j.mseb.2022.115881
- [43] S.D. Dhas, P.S. Maldar, M.D. Patil, A.B. Nagare, M.R. Waikar, R.G. Sonkawade, A.V. Moholkar, Vacuum 181 (2020) 109646;
- https://doi.org/10.1016/j.vacuum.2020.109646
- [44] M. Danish, A. Mehmood, Z.A. Sandhu, M. Asam Raza, S. Ashraf, F. Ali, A.H. Bhalli, M. Aslam, K.M. Batoo, M.F. Ijaz, Physica Scripta (2024); https://doi.org/10.1088/1402-4896/ada30d
- [45] M. Danish, A. Ashraf, Z.A. Sandhu, M.A. Raza, A.H. Bhalli, A.G. Al-Sehemi, Journal of Molecular Structure 1294 (2023) 136296; https://doi.org/10.1016/j.molstruc.2023.136296
- [46] M. Danish, S. Akram, Z.A. Sandhu, A. Akhtar, A.A. Altaf, S. Ullah, A. Ali, M.A. Raza, Journal of Inorganic and Organometallic Polymers and Materials 33(9) (2023) 2803-2813; https://doi.org/10.1007/s10904-023-02719-4
- [47] H.S. Magar, R.Y. Hassan, A. Mulchandani, Sensors 21(19) (2021) 6578; https://doi.org/10.3390/s21196578